DOI: 10.17725/rensit.2021.13.369

Graphene-polyethylene high pressure composites and their properties

Ekaterina G. Rustamova
SPO "GRAPHENIKA", https://www.grafenika.com/
Moscow 107143, Russian Federation
Sergey P. Gubin
N.S. Kurnakov Institute of General and Inorganic Chemistry of RAS, http://www.igic.ras.ru/
Moscow 119991, Russian Federation
E-mail: nebukina@yandex.ru, gubin@igic.ras.ru
Received July 28, 2021, peer-reviewed August 09, 2021, accepted August 23, 2021

Abstract: **A method for the introduction graphene into high-pressure polyethylene (HPPE) has been developed. Samples of graphene-HPPE were obtained with the content of graphene filler: 0.25%; 0.5%; 1.0%; 1.5%; 3.0%; 5.0% wt. The structural, morphological and deformation-strength properties of the obtained samples have been investigated. It was established that the increase of the elastic modulus value for the samples with the filler concentration of 3% wt and more.**

Keywords: **graphene, high-pressure polyethylene, polymeric nanocomposite materials**

UDC 54.03'05'06

Acknowledgments: The authors express their gratitude and deep appreciation to the staff of the Laboratory of Inorganic and Hybrid Polymers and Composites at the Semenov Institute of Chemical Physics, Russian Academy of Sciences for the help in the investigation of the rheological and deformation-strength properties of graphene-HPPE composites.

For citation: Ekaterina G. Rustamova, Sergey P. Gubin. Graphene-polyethylene high pressure composites and their properties. *RENSIT*, 2021, 13 (3):369-376. DOI: 10.17725/rensit.2021.13.369.

Contents

1. INTRODUCTION

Currently, nanocomposites represent a new direction in the field of filled systems. Due to the special properties of nanoscale fillers, the most attention of scientists is focused on the development of polymer nanocomposite materials [1-5].

Carbon nanostructures, and graphene in particular, are promising fillers, which attract the special interest of researchers..

Graphene is a two-dimensional unit layer of carbon, only one sp^2-carbon atom thick and has many unique physical properties [6-13]. Experimental data show that the values of Young's modulus – 1 TPa, the maximum current density – 10^8 A·cm^{-2}, the coefficient of thermal conductivity of up to 5000 m^{-1}K^{-1}, the charge carrier mobility at room temperature of 10^4 cm^{2}K^{-1s-1}[14-17].

Due to the introduction of a graphene filler into various polymers, the obtained composites acquire improved characteristics in terms of strength, rigidity, electrical and thermal conductivity [18-20].

In turn, high-pressure polyethylene (HPPE) is one of the most common, widely available and cheap polymers, the expansion of the areas of

its application by modifying its properties is a currently important direction.

In this regard, the aim of this work was to develop a method of introducing graphene into high-pressure polyethylene, to obtain polymer composites of graphene-HPPE, and to study their properties.

2. EXPERIMENTAL

The following were used as precursors for the synthesis of graphene and composite materials: Chinese natural graphite (99.9% C, crushed in a ball mill to a size of 200-300 μm), sulfuric acids (ACS, "Sigma Tech" LLC), potassium permanganate (p.a., "NevaReaktiv" LLC), hydrogen peroxide (p.a., "NevaReaktiv" LLC), isopropyl alcohol (ACS, "EKOS-1" JSC), high pressure polyethylene (CAS-No: 9002-88-4, Sigma Aldrich), vacuum oil BM1 (industry standard OST 38.101402-86, "GSM Group" LLC), distilled water.

The samples of the graphene-HPPE composites were obtained in two stages. At the first stage graphene was synthesized. For this purpose, the natural graphite used as a starting material, was oxidized to graphite oxide by a modified Hummers' method [21-23]. The obtained oxidized product was dispersed in distilled water using an ultrasonic unit (20.4 kHz frequency, 0.1–1 W/cm^3 specific power) for 15 minutes until formation of graphene oxide. After that, the aqueous dispersion was centrifuged (6000 rpm for 10 min), a precipitate was isolated and dried at a temperature of 60°C for 24 h. Then, the powdered graphene oxide was reduced to graphene with isopropanol under supercritical conditions [24].

At the second stage the obtained graphene was dispersed in isopropyl alcohol in the ratio of 1mg/1ml for 1 h by ultrasonic treatment. The obtained graphene dispersion was introduced in small portions into solution-melt HPPE-BM1 oil at a temperature of 200°C under the condition of constant stirring (1200 rpm). The removal of isopropanol vapors from the reaction vessel was carried out by an argon flow.

At the end of the synthesis, the reaction mixture was cooled to room temperature. The obtained composite was purified from oil by extraction with hexane in a Soxhlet's apparatus for 16 h.

Thus, the samples of graphene-HPPE containing 0.25, 0.5, 1, 1.5, 3 and 5% wt of graphene, which are powders, were obtained. **Fig. 1** shows a sample of the graphene-HPPE composite containing 5 wt.% of graphene.

By the method of hot pressing from the samples, with different content of the carbon filler, the films were obtained. For this purpose, powdered samples (m = 5 g) were evenly distributed over the volume of copper frames (100×100×0.041 mm) and kept for 30 sec at 180°C and pressure of 20 kg/cm^2. Fixation of the shape of the products occurred as a result of cooling the samples to room temperature.

The structural characteristics of the samples were investigated using powder diffractometry and Raman spectroscopy. *X*-ray phase analysis (XRD) was carried out on DRON-7 unit with graphite monochromator on CuKα-radiation

Fig. 1. *A sample of the graphene-HPPE composite.*

(λ = 1.54056 Å) with Ni filters. The Raman spectroscopy signals were recorded using a photomultiplier (PMT) operating in the photon counting mode. The spectra were accumulated on a personal computer.

The morphology of graphene flakes in isopropanol and in a HPPE matrix was determined by analytical processing of microphotographs obtained by transmission electron microscopy (TEM) on a Leo 912 AB Omega unit at an accelerating voltage of 100 kV.

Before imaging, the samples were placed on carbon-film-coated copper grids 3.05 mm in diameter. Translucent images were acquired at magnifications up to 500,000×. A restriction aperture with a diameter of 0.4 μm was used to obtain electron diffraction images.

Atomic force microscopy (AFM) was used to determine the lateral size and height of the graphene particles. The samples were imaged using a Solver P47 microscope (Solver scanner, sonde NSG01) at a nominal cantilever resonance frequency of 150 kHz, cantilever stiffness constant of 5.1 N/m, sonde radius of 10 nm, scanning speed of 1 Hz, and resolution of 512x512 points.

Before the AFM study, a 10 *μl* drop of graphene dispersion in isopropanol was placed on freshly pierced mica and incubated at room temperature until complete evaporation of the solvent.

Deformation-strength studies of graphene-HPPE samples were performed on an Instron 5540 series testing machine. Blades of standard sizes (11×80 mm) were cut from the manufactured graphene-HPPE composite films and tested at room temperature, pressure of 620 kPa, and speed of 50 mm/min.

The rheological properties of the samples of graphene-HPPE composites were studied using a capillary viscometer.

3. RESULTS AND DISCUSSION

Before the introduction of graphene, obtained from natural graphite by chemical processes (oxidation, dispersion, reduction), into high pressure polyethylene, it was characterized by a complex of methods of physical and chemical analysis.

X-ray phase analysis (XRF) and Raman spectroscopy were used to obtain data on the structure of graphene.

The diffractogram of the initial graphite (**Fig. 2***a*) shows characteristic reflexes of low (at the angles of 2θ: 12.5, 25, 55 deg) and strong intensity (at 2θ – 26.6 deg) corresponding to the graphite phase with the hexagonal lattice structure.

The transition from the densely packed, compact source material to the nano-object, graphene, resulted in a decrease in the intensity and significant broadening of the diffraction maximum in the region of 26.6 deg. (Fig. 2*b*). In addition, there is a disappearance of low-intensity reflexes characteristic of graphite. These results indicate an increase in the sample dispersion (reduction of the size of graphene particles).

Additional information about the graphene structure was obtained using Raman spectroscopy. Raman spectroscopy is a powerful tool for the identification of non-destructive carbonaceous materials, in particular, for the determination of ordered and disordered crystal structures of carbon.

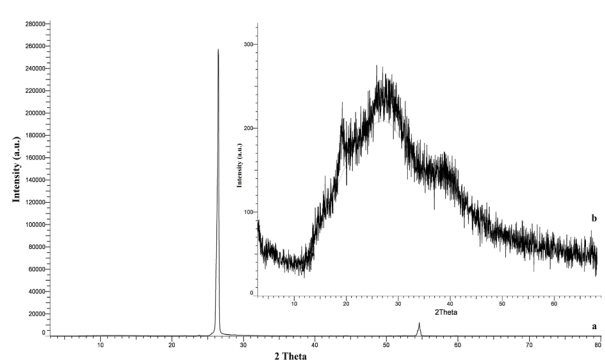

Fig. 2. *Diffractograms of samples: a - original graphite, b - graphene.*

G (≈1582cm^{-1}) and *D* (≈1350cm^{-1}) lines are characteristic features for carbon in Raman scattering spectra. The *G*-line is usually attributed to the E_{g2} phonon sp^2-hybridized carbon atoms, whereas the *D*-line constitutes the fully symmetric valence vibration $\varkappa$-point phonons of A_{1g} symmetry [25-28]. The overtones of these lines are 2*G* and 2*D*, located at 3248 cm^{-1} and 2700 cm^{-1} respectively.

The Raman spectrum of natural graphite (**Fig. 3***a*), used as a feedstock for graphene production, is represented by a strong *G*-line (1582 cm^{-1}), a broad 2*D*-line (2700 cm^{-1}), and a very weak 2*G* line at 3245 cm^{-1}. In the Raman spectrum signals of graphene (Fig. 3*b*), the *G* band broadens and shifts to 1590 cm^{-1}, an intense *D* band at 1350 cm^{-1} appears, there is a slight shift of the 2D and disappearance of the 2*G* bands. These phenomena can be attributed to the significant size reduction in the sp^2 plane of the domains due to exfoliation of the graphite crystal structure by oxidation and ultrasonic treatment to graphene oxide followed by its reduction [29,30].

The morphology of graphene was analyzed by transmission electron microscopy. Microphotographs show graphene sheets with a thin, transparent, slightly folded structure, resistant to the electron beam action.

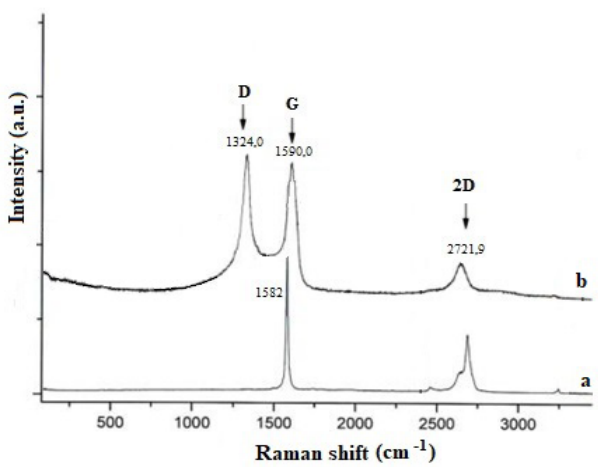

Fig. 3. *Raman spectrum: a-graphite, b-graphene.*

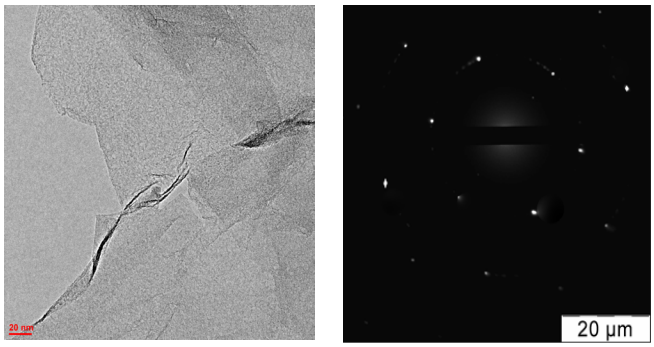

Fig. 4. *TEM image and electron diffraction of graphene.*

Electron diffraction was performed from the selected area of the graphene particle. **Fig. 4** shows the diffraction pattern in which clearly defined point reflexes confirm the crystalline structure of the graphene sheets.

By the AFM method the geometric parameters of the studied graphene were established. The AFM images show flat particles with lateral sizes from 1.5 to 3 μm and thickness of 1-2 nm, which corresponds to 3-5 layers of graphene. **Fig. 5** shows a single sheet of graphene.

After the basic structural and morphological characteristics of graphene were found out, it was used as a nanofiller for polyethylene.

High-pressure polyethylene has a rather rigid and complex structure, consisting of molecules, tightly stacked in parallel one to another to form lamellae. The introduction of graphene into the polymer could be accompanied by aggregation and uneven distribution of the filler particles, due to their difficult penetration between the lamellae.

In order to "activate" polyethylene, i.e. to make its structure available for the introduction and uniform fixation of the graphene particles,

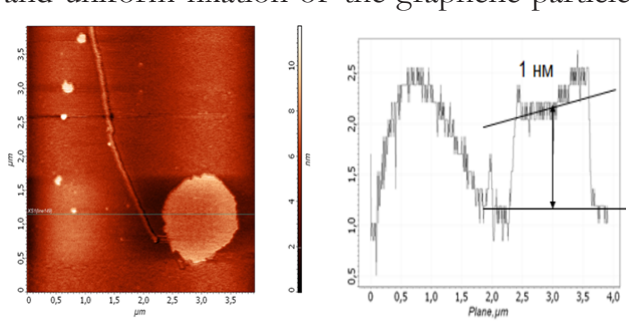

Fig. 5. *AFM–image and cross-section of a graphene sheet.*

vacuum oil was used. Vacuum oil mixed well with polyethylene, allowed to move apart the lamellae and create a very mobile reaction environment, allowing the filler to freely penetrate into the structure of polyethylene.

The obtained samples of graphene-HPPE in powder form contained from 0.25 to 5 wt% of the graphene filler and differed little from each other in color. However, after transforming the powders into films, a gamma from light to dark gray hue was formed. The degree of color saturation of the samples increased with increasing concentration of graphene in the HPPE.

Fig. 6 shows the TEM-image of the graphene-HPPE sample. The microphotograph shows a curved graphene sheet with lateral dimensions of 2 μm, which has entered the polymer structure. The authors of [31] argue that the surface relief and twisting are inherent to the graphene sheets, as the thermodynamic stability of the 2*D* structures occurs as a result of microscopic folds due to bending and deformation.

The electronogram (Fig. 6) for this sample is represented by blurred weakly pronounced ring reflexes due to the amorphous component of the polymer and signals in the form of single points characterizing the graphene crystal structure.

The results of Raman-spectra study of HPPE samples without the filler and with it showed that the filler introduction into the polymer is

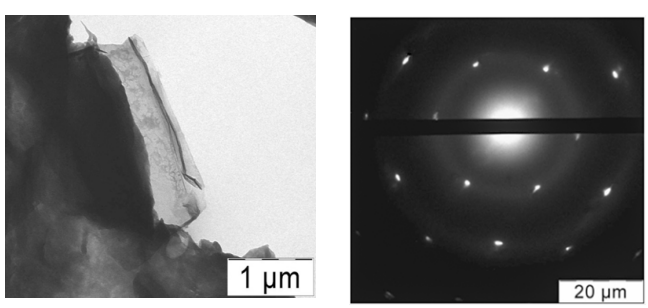

Fig. 6. *TEM-image and electron diffraction of the graphene-HPPE composite sample.*

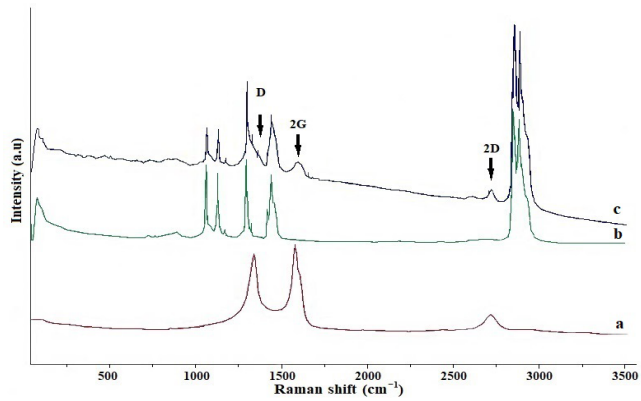

Fig. 7. *Image of the Raman spectroscopy of the studied samples: a - graphene, b - HPPE, c - graphene-HPPE composite.*

accompanied by the appearance of *G, D* and 2*D* lines typical for the carbon structures in the Raman spectra (**Fig. 7**).

Further stage of the work consisted in the study of the graphene-HPPE film samples properties.

Fig. 8 shows the results of the study of the films surface using an optical microscope. The image (Fig. 8) shows a uniform distribution of the filler particles of large (5-10 microns) and small (1-2 microns) size. Besides, the presence of light strips - defects (microcracks) is noted on the surface of the films.

A possible reason for such defects may be the presence of macroparticles located at the boundary of the crystallites, which behave as stress concentrators and contribute to the film surface continuity breaking.

The measurement of the deformation-strength characteristics of the graphene-HPPE nanocomposites made it possible to obtain the

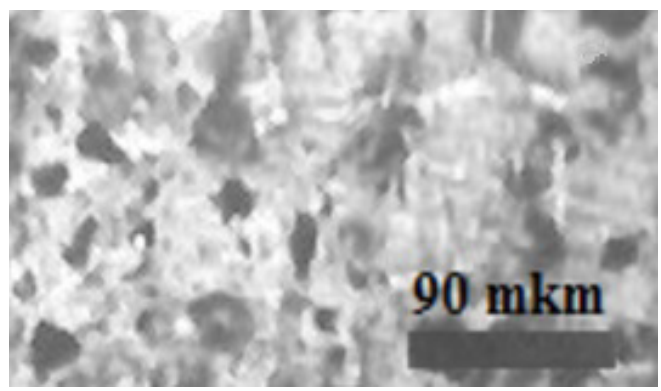

Fig. 8. *Image of the graphene-HPPE film surface.*

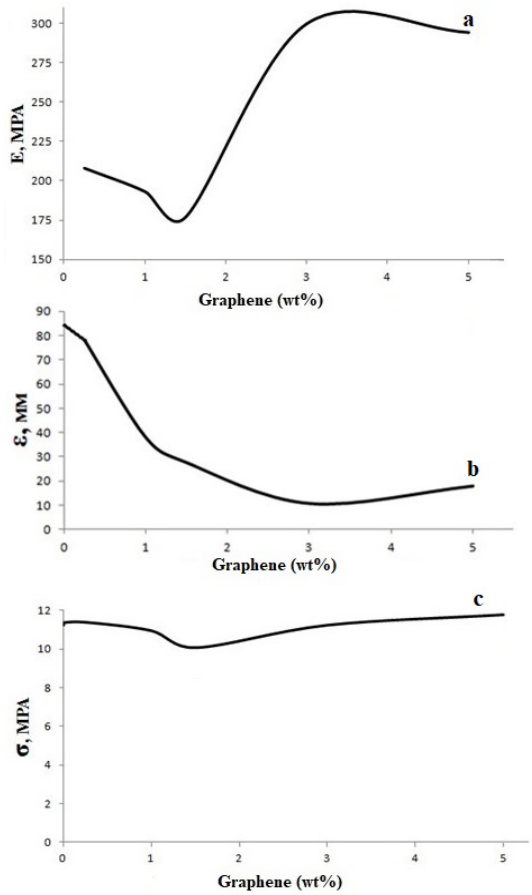

Fig. 9. *Concentration dependences: a - elastic modulus, b - elongation at break, c - strength of the graphene-HPPE samples.*

concentration dependences of the strength, modulus of elasticity, and elongation at rupture for the samples under study (**Fig. 9**).

According to the above presented data, the strength and elongation at break of the graphene-HPPE composites decrease, which is typical for the introduction of rigid anisotropic particles into polyolefin polymers.

The values of the elastic modulus remain unchanged for the samples with the filler concentration up to 1,5 wt.% and increase by 100 MPa at the graphene filling by 3% and more wt.%.

In addition to the deformation-strength characteristics for the graphene-HPPE samples, the rheological properties were studied.

Fig. 10 shows the flow curves of the studied samples. There is a directly proportional growth of the composites' viscosity with the increase

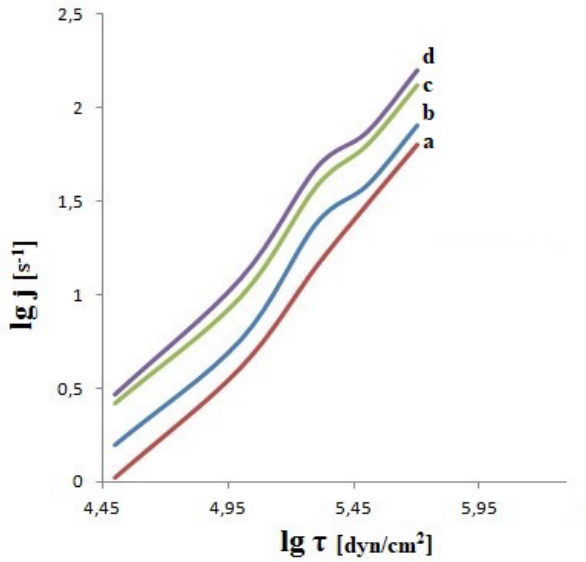

Fig. 10. *Flow curves of graphene-HPPE composite samples: a - HPPE, b - graphene- HPPE (1.5% wt.), c - graphene-HPPE (3% wt.), d - graphene-HPPE (5% wt.)*

in the graphene concentration from 1.5 to 5 wt.%. For the samples of graphene-HPPE with a lower filler content the values of the measured characteristics are comparable with the result obtained for HPPE without graphene. The viscosity growth is accompanied by the increase in the pseudomolecular weight of the graphene-HPPE samples. It is possible that this effect can be due to the increased interaction of the graphene sheets with the carbon chains of polyethylene.

4. CONCLUSION

During the conducted research work the method of graphene introduction into polyolefin polymer was developed, the samples of graphene-HPPE with different filler content (0.25-5 wt.%) were obtained. The structural and morphological characteristics of the graphene and the composite material were studied. Strain-strain characteristics of graphene-HPPE composite films with the thickness of 41 microns were measured and their rheological properties were investigated. It was found that the ultimate strength of the samples does not depend on the filler concentration, while the increase in its content in the composites leads to a decrease in the value of the relative elongation. There

is an increase in the elastic modulus relative to the values obtained for polyethylene without the filler by 100 mPa for the graphene-HPPE samples at the concentration of graphene 3 and more wt%. The results of the study of the rheological properties of the graphene-HPPE films, led to the conclusion about the growth of the interaction of graphene sheets with the carbon chains of polyethylene.

REFERENCES

1. Krishnamoorti R, Vaia RA. Polymer nanocomposites. J*ournal of Polymer Science Part B: Polymer Physics,* 2007, 45(24):3252–3256.
2. Jordan J, Jacob KI, Tannenbaum R, Sharaf MA, Jasiuk I. Experimental trends in polymer nanocomposites - a review. *Materials Science and Engineering: A*, 2005, 393:1–11.
3. Kim H, Abdala AA, Macosko CW. Graphene/Polymer Nanocomposites. *Macromolecules,* 2010, 43:6515-6530.
4. Nikolaichik VI, Gertsen MA, Avilov AS, Kornilov DY, Gubin SP. Pentagonal cobalt boride nanoparticles on the polystyrene granule surface. *Crystallography Reports,* 2019, 64(3):461-465.
5. Yasnaya MA, Kornilov DYu, Sytnikov EV, Sinel'nikov BM, Kargin NI, Khoroshilova SE. Metal-polymer nanocomposites as materials for ion-selective sensors. I*norganic Materials*, 2008, 44(3):230-238.
6. Novoselov KS, Geim AK, Morozov SV, Jiang D, Zhang Y, Dubonos SV, Grigorieva IV, Firsov AA. Two-dimensional gas of massless Dirac fermions in graphene. *Science,* 2004, 306:666-669.
7. Worsley MA, Olson TY, Lee JR. High surface area, sp^2-cross-linked three-dimensional graphene monoliths. *The Journal of Physical Chemistry Letters,* 2011, 2(8):921-925.
8. Papageorgiou DG. Mechanical properties of graphene and graphene-based nanocomposites. *Progress in Materials Science,* 2017, 90:75-127.
9. Babaev AA, Zobov ME, Kornilov DY, Tkachev SV, Terukov EI, Levitskii VS. Temperature dependence of electrical resistance of graphene oxide. *High Temperature,* 2019, 57(2):198-202.
10. Babaev AA, Zobov ME, Kornilov DY, Tkachev SV, Terukov EI, Levitskii VS. Specific features of temperature dependence of graphene oxide resistance. *Protection of Metals and Physical Chemistry of Surfaces,* 2019, 55(1):50-54.
11. Babaev AA, Zobov ME, Kornilov DY, Tkachev SV, Terukov EI, Levitskii VS. Optical and electrical properties of graphene oxide. *Optics and Spectroscopy,* 2018, 125(6):1014-1018.
12. Rychagov AY, Gubin SP, Chuprov PN, Kornilov DY, Karaseva AS, Krasnova ES, Voronov VA, Tkachev SV. Electrochemical reduction and electric conductivity of graphene oxide films. *Russian Journal of Electrochemistry,* 2017, 53(7):721-727.
13. Zaytsev EV, Bukunov KA, Bocharov GS, Chuprov PN, Tkachev SV, Kornilov DYu, Kurkina E S, Gubin SP, Eletskii AV. Graphene microtubes - new type of carbon materials. *RENSIT*, 2018, 10(1):59-64.
14. Mudryan VE, Sokolov EA, Piven NP, Babenko SD, Allayarov SR Anomalous behavior of the dielectric constant of a polymer composite with the addition of graphene. *ZhTF Letters,* 2010, 36(23):106-110.
15. Ferrari A et al. Science and technology roadmap for graphene, related two-dimensional crystals, and hybrid systems. *Nanoscale,* 2015, 7:4598-4810.
16. Wick P. Classification framework for graphene-based materials. *Chem. Int. Ed,* 2014, 53:7714-7718.
17. Bianco A. All in the graphene family - a recommended nomenclature for two-dimensional carbon materials. *Carbon*, 2013, 65:1-6.

18. Huang G, Gao J, Wang X, Liang H, Ge C. How can graphene reduce the flammability of polymer nanocomposites? *Materials Letters,* 2012, 66:187-189.
19. Zaitsev EV, Chuprov PN, Tkachev SV, Kornilov DY, Gubin SP, Kurkina ES, Bocharov GS, Eletskii AV. Preparation of graphene on copper substrates of various geometries by chemical vapor deposition. *Inorganic Materials*, 2018, 54(12):1205-1215.
20. Tkachev SV, Kornilov DY, Voronov VA, Gubin SP, Kraevskii SV. Graphene oxide on the surface of basalt fiber. *Inorganic Materials,* 2016, 52(12):1254-1258.
21. Hummers WS, Offeman RE. Preparation of graphitic oxide. *J. Am. Chem. Soc*, 1958, 80:1339.
22. Kornilov DY, Gubin SP. Graphene Oxide: Structure, Properties, Synthesis, and Reduction (A Review). *Russ. J. Inorg. Chem*, 2020, 65:1965-1976.
23. Yang D Chemical analysis of graphene oxide films after heat and chemical treatments by x-ray photoelectron and micro-Raman spectroscopy. *Carbon*, 2009, 47:45-52.
24. Tkachev SV, Buslaeva EYu, Gubin SP. Graphene: A novel carbon nanomaterial. *Inorg. Mater*, 2011, 47(1):1.
25. Tuinstra F. Koenig JL. Raman spectrum of graphite. *J. Chem. Phys*, 1970, 53:1126-1130.
26. Ferrari AC, Robertson J. Interpretation of Raman spectra of disordered and amorphous carbon. *Phys. Rev. B*, 2000, 61:14095-14107.
27. Ni Z, Wang Y, Yu T. et al. Raman spectroscopy and imaging of graphene. *Nano Res*, 2008, 1:273-291.
28. Muzyka R, Drewniak S, Pustelny T, Chrubasik M, Gryglewicz G. Characterization of graphite oxide and reduced graphene oxide obtained from different graphite precursors and oxidized by different methods using Raman spectroscopy. *Materials,* 2018, 11:1050.
29. Wang G, Yang J, Park J, Gou X, Wang B, Liu H. et al. Facile synthesis and characterization of graphene nanosheets. *J. Phys. Chem. C*, 2008, 112:8192–8195.
30. Kornilov DY, Kasharina LA. Effect of preparation and reduction on specific surface electrical resistance of thin films obtained from graphene oxide dispersion. *Inorganic Materials: Applied Research,* 2019, 10(5):1072-1077.
31. Meyer JC, Geim AK, Katsnelson MI, Novoselov KS, Booth TJ. Roth S. The structure of suspended graphene sheets. *Nature,* 2007, 446:60-63.